Supplement of Ocean Sci., 22, 3771–3793, 2026
https://doi.org/10.5194/os-22-3771-2026-supplement
© Author(s) 2026. CC BY 4.0 License.



Ocean Science Open Access EGU

Supplement of

First global assessment of the Eddy-Diffusivity Mass-Flux (EDMF) parameterization for oceanic convection in NEMO: implications for global temperature and surface heat fluxes

Violaine Piton et al.

Correspondence to: Violaine Piton (vpiton@mercator-ocean.fr)

The copyright of individual parts of the supplement might differ from the article licence.

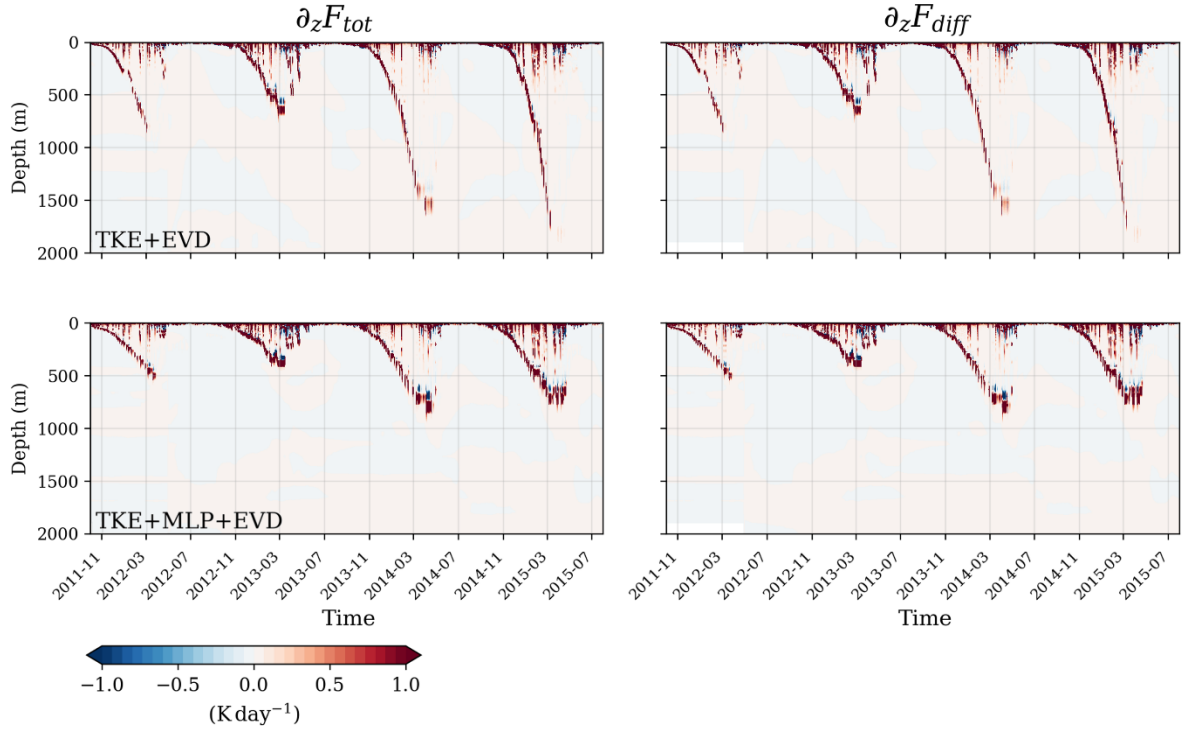


Figure S1: Vertical divergence (K day^{-1}) of the total ($\partial z F_{tot}$) and diffusive ($\partial z F_{diff}$) vertical heat fluxes at the model grid cell containing the Labrador Sea mooring (56.53°, 52.65°W), over the same period as shown in Fig. 2a, for TKE+EVD (first row) and TKE+MLP+EVD (second row) simulation computed from daily model outputs.

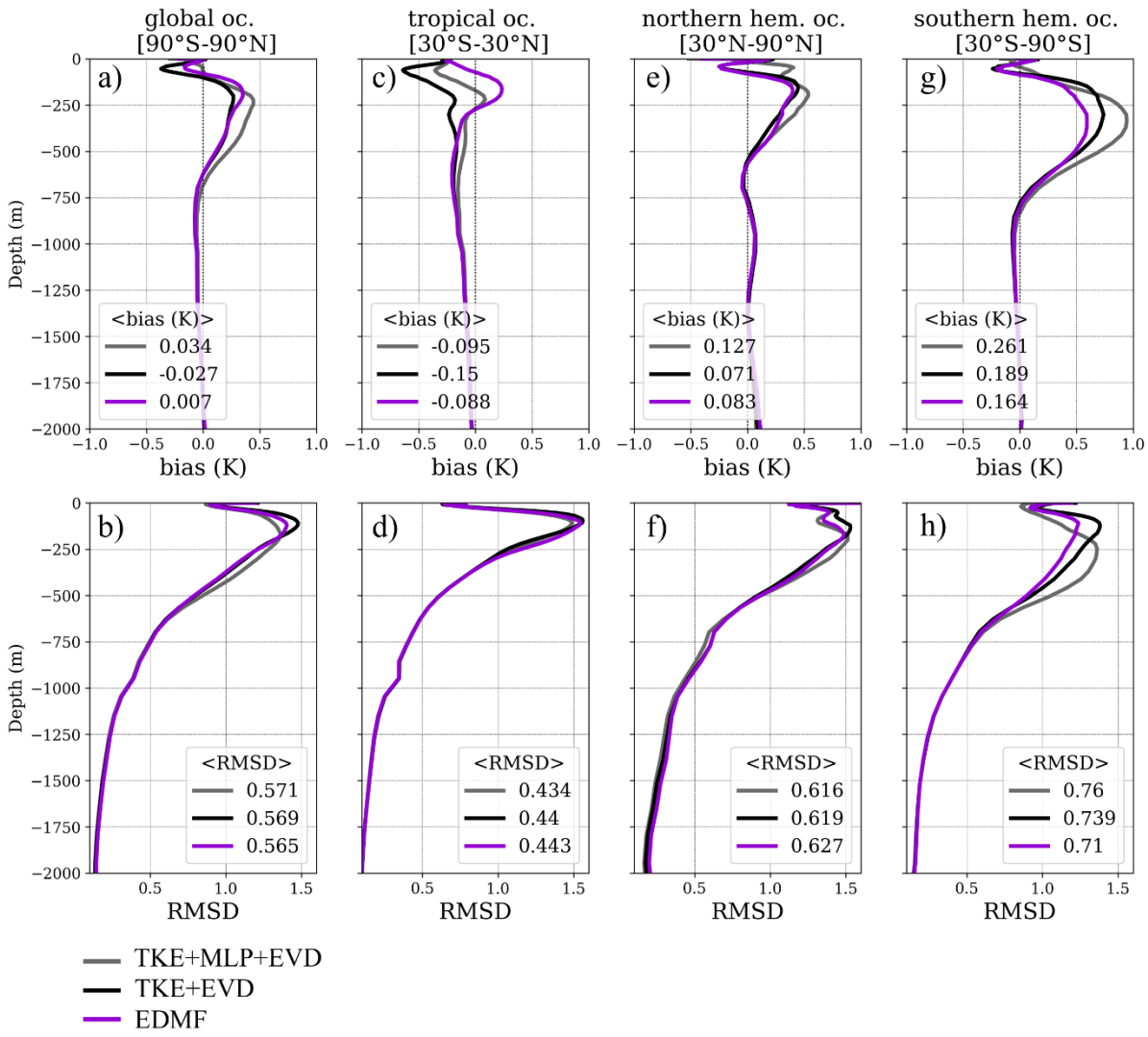


Figure S2: 0 to 2000-m depth profiles of temperature bias (difference between the simulation and the observation; top row) and corresponding RMSD (bottom row) for the three simulations, averaged over the 2005-2020 period for the global ocean (a,b), for the tropical ocean (c,d), for the northern hemisphere ocean (e,f) and for the southern hemisphere ocean (g,h). 0 -2000 m depth-averaged values of bias and RMSD are provided for each profile in the corresponding legend box.

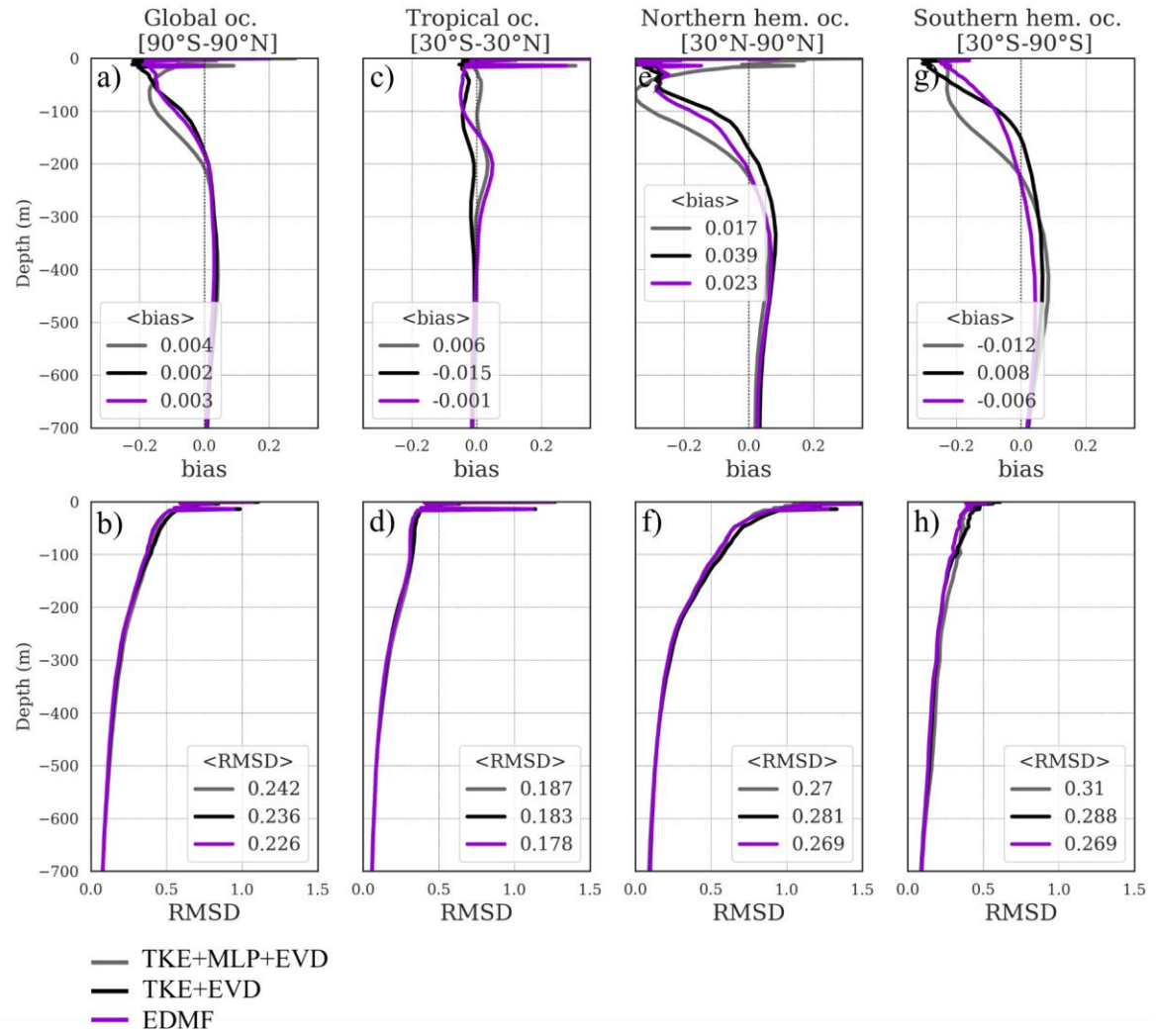


Figure S3: 0 to 700-m depth profiles of salinity bias (difference between the simulation and the observation; top row) and corresponding RMSD (bottom row) for the three simulations, averaged over the 2005-2020 period for the global ocean (a,b), for the tropical ocean (c,d), for the northern hemisphere ocean (e,f) and for the southern hemisphere ocean (g,h). 0 -700 m depth-averaged values of bias and RMSD are provided for each profile in the corresponding legend box

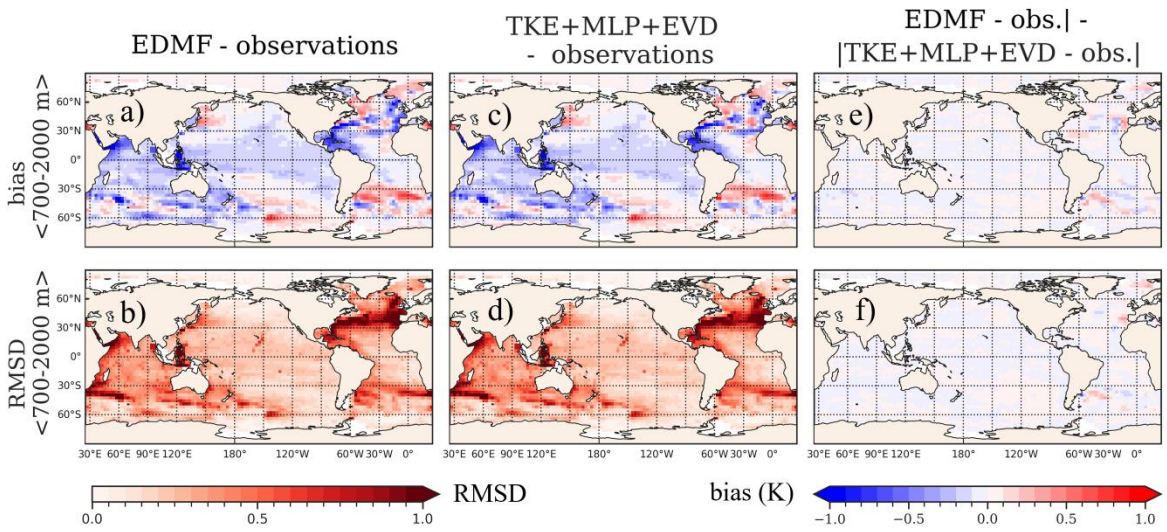


Figure S4: Maps of depth-averaged temperature bias from 700 to 2000 and associated RMSD between EDMF and the observations (a,b) and TKE+MLD+EVD and the observations (c,d).

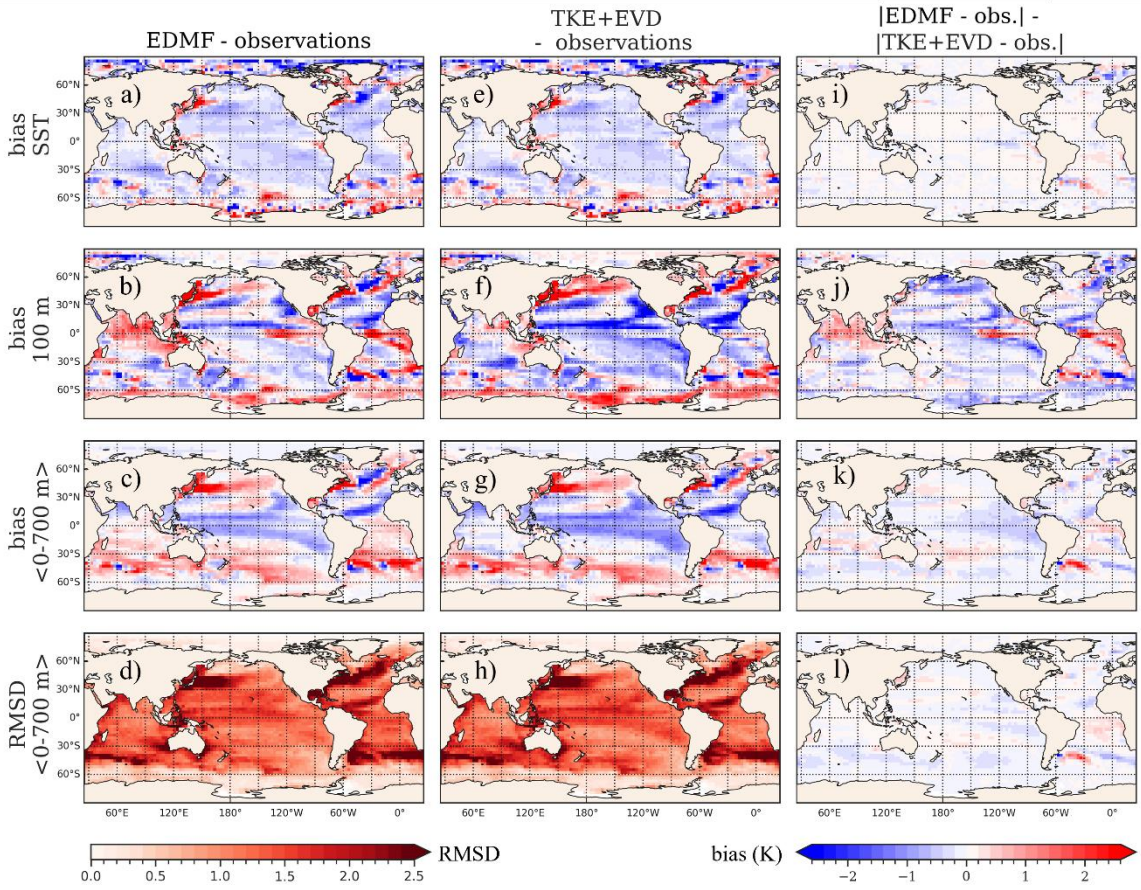


Figure S5: (a-d) Maps of bias between the EDMF simulation and the observations for SST (first row), temperature at 100 m (second row), depth-averaged temperature between 0 and 700 m (third row) and the corresponding 0-700 m averaged RMSD (fourth line). (e-h) Same as (a-d) but for the TKE+EVD simulation. (i-l) Maps of absolute differences between the biases for the three depth ranges considered, and (i) the corresponding RMSD differences.

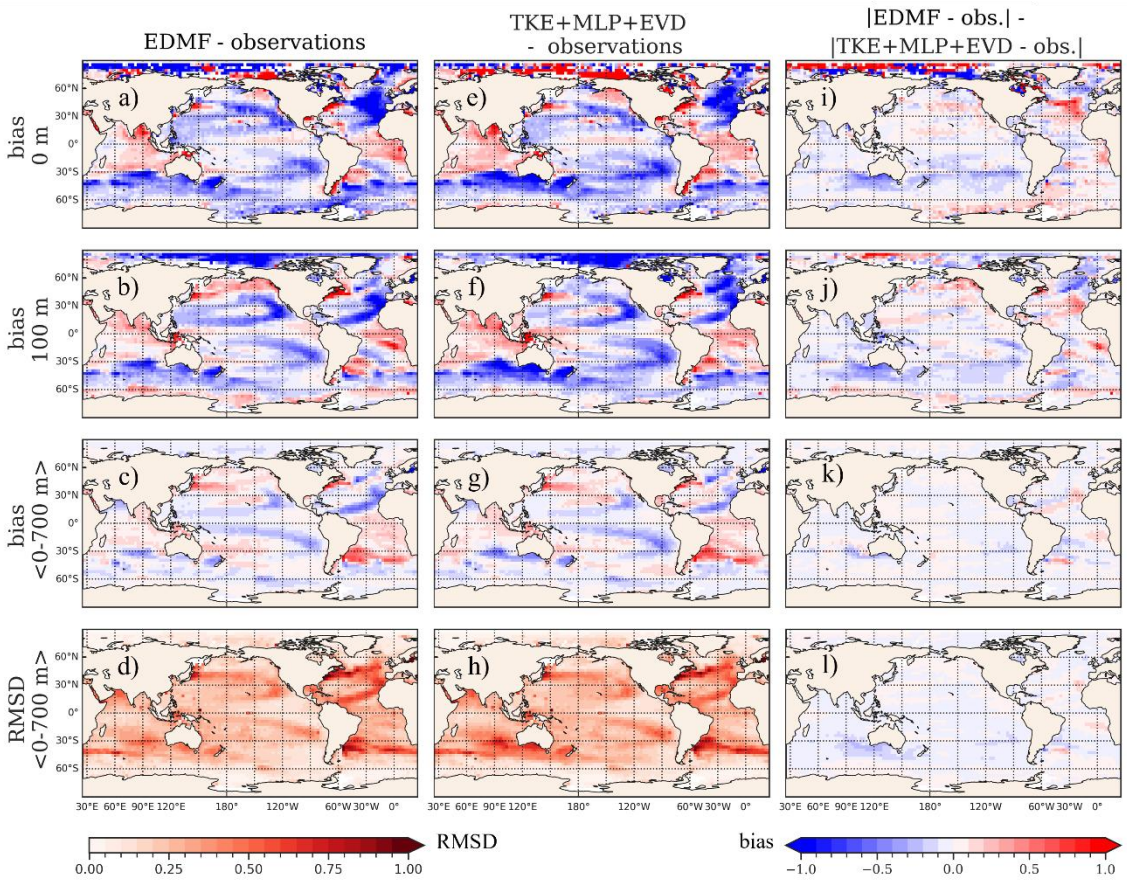


Figure S6: (a-d) Maps of bias between the TKE+EDMF simulation and the observations for surface salinity (first row), salinity at 100 m (second row), depth-averaged salinity between 0 and 700 m (third row) and the corresponding RMSD (fourth line). (e-h) Same as (a-d) but for the TKE+MLD+EVD simulation. (i-k) Maps of absolute differences between the biases for the three depth ranges considered, and (l) the corresponding RMSD differences.

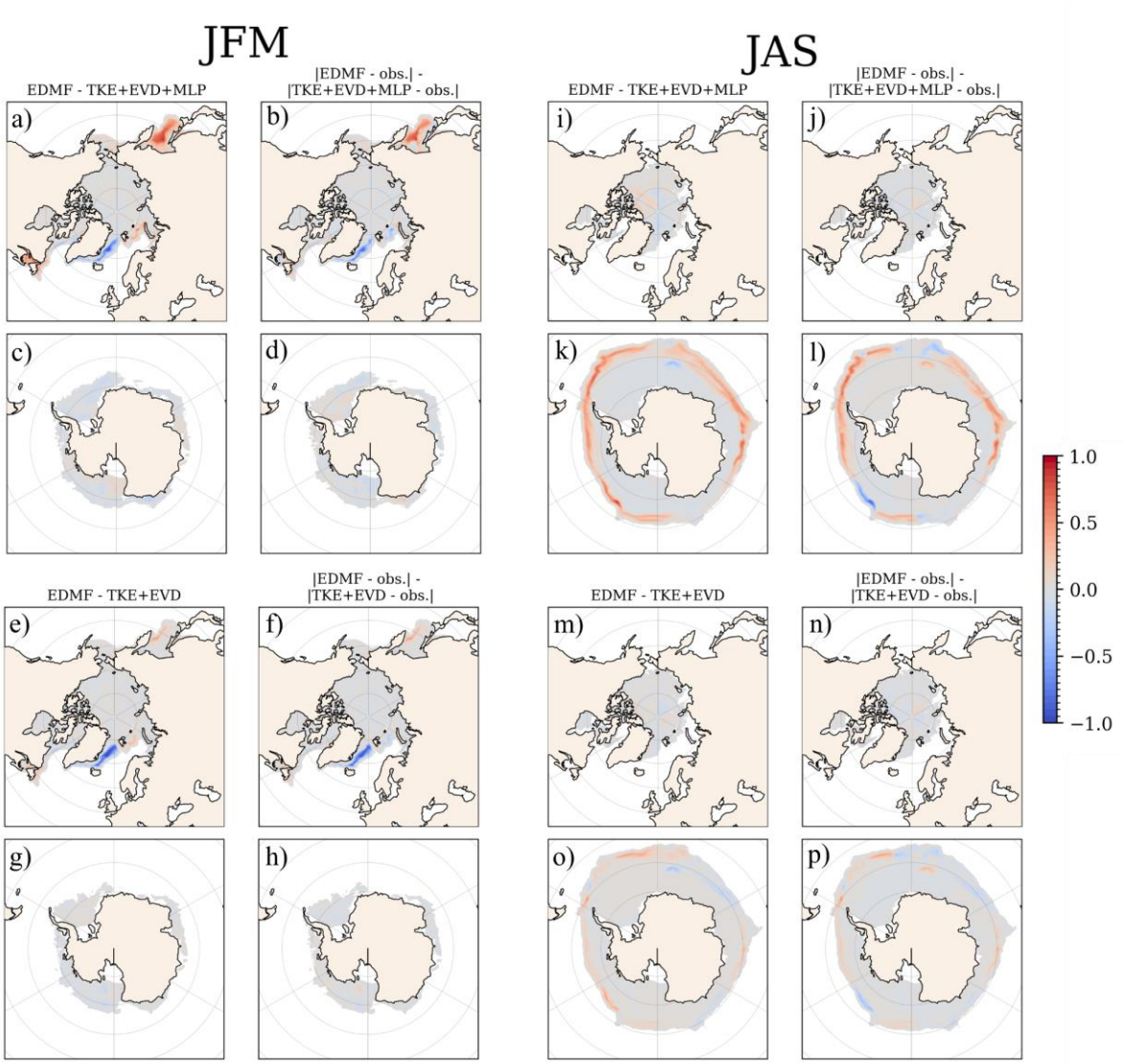


Figure S7: JFM and JAS maps of differences in sea-ice concentration between EDMF and TKE+EVD+MLP simulations (a, c, i, k) and between EDMF and TKE+EVD (e, g, m, o) for the Arctic and Antarctic regions, and corresponding maps of absolute differences in sea-ice concentration (b, d, j, l, f, h, n, p).

S1. AMOC observational dataset and transport analysis

We compare the modeled Atlantic Meridional Overturning Circulation (AMOC) with the observed RAPID-MOCHA monitoring array at 26.5°N, which monitored the AMOC volume transport since April 2004 (https://rapid.ac.uk/data). The modeled AMOC computations are performed with the cdftools package (cdfmoc; https://meom-group.github.io/doc/CDFTOOLS/#PACKAGE-DESCRIPTION).

The simulations performances are evaluated for the Atlantic meridional overturning circulation *(*AMOC), a climate relevant quantity that ocean models aim to simulate accurately. All simulations underestimate the annually averaged AMOC transport along the RAPID section at 26.5°N and fail to reproduce the observed trend (Fig. S7). Overall, the

transport values from the EDMF simulation fall within the range of the other two simulations, suggesting a reasonable representation of the AMOC by the EDMF simulation. However, such underestimations of transport are a common feature in global circulation models and are likely linked to reduced transport of Lower North Atlantic Deep Water (Bryden et al., 2024).

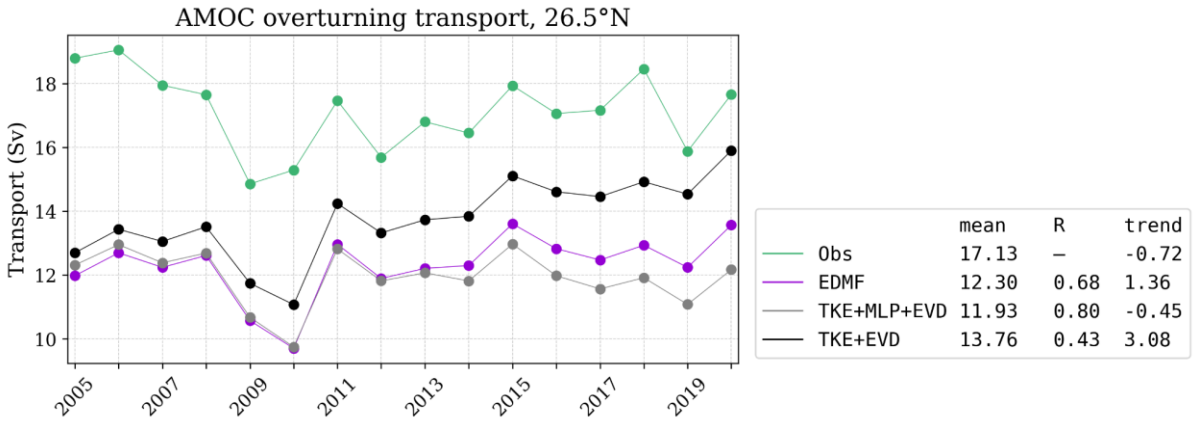


Figure S8: Yearly time series of Atlantic meridional overturning circulation (AMOC) transport (in Sv) from observation (green), the EDMF (purple), the TKE+EVD (black) and the TKE+MLP+EDMF (gray) simulation. The legend indicates the mean (in Sv), the correlation coefficient (R) between each simulation and the observations and the trend (in Sv) for each dataset over the 16-year period.

S2. Observational dataset for sea-ice concentration

Seasonal modelled sea-ice concentration for the Arctic and Antarctic regions are compared to the GCOM-W1 product (Global AMSR Sea Ice Concentration, OSI SAF, 2017; https://dx.doi.org/10.15770/EUM_SAF_OSI_NRT_2023) derived from AMSR-2 satellite measurements and processed by the EUMETSAT OSISAF.